Space-Time Ground Diffusion: The ATL Law for Accelerators

Vladimir Shiltsev*
DESY-MPY, Notkestrasse 85, 22603 Hamburg, GERMANY
e-mail: shiltsev@x4u2.desy.de

November 16, 1995

Abstract

This article presents an overview of diffusive ground motion and its consequences for accelerators. Numerous measurements are reviewed where diffusion was detected at the lowest limit of background for seismic motion. Experimental investigations carried out at accelerator facilities and at geophysical laboratories, with various types of equipment and with different approaches show that this residual diffusive motion can often be approximated by "the *ATL law*". The latter predicts that ground points perform Brownian motion characterized by the variance of the relative displacement which scales as a product of temporal and spatial intervals. The model gives some predictions of continuously reproducible charged-particle-beam distortions due to misalignment for future linear colliders and other large accelerators.

1 Introduction

1.1 The ATL Law

The *ATL law* was originally proposed in 1991 in Ref.[1, 2] and developed in Ref.[3] to describe experimental data on the relative displacement of two distant ground points. According to this empirical rule, the rms relative displacement dX of two points located at a distance *L* grows with time T:

$$< dX^2 >= ATL, \tag{1}$$

where *A* is a constant of the order of $10^{-5\pm1}\mu m^2/(s\cdot m)$ that depends on the site. The diffusion wandering of the ground elements takes place in all directions.

As long as the diffusive coefficient *A* is small the wandering presents only a tiny contribution to the ground motion. For example, in the time period of 1 hour the amplitude of

*on leave from Budker Institute of Nuclear Physics, 630090, Novosibirsk, RUSSIA

the absolute surface motion (measured by seismometer) is of the order of $100\mu\mathrm{m}$, while the *ATL* estimation gives about $1\mu\mathrm{m}$ for points 30 m apart. One would not worry about this contribution except it describes very important, at least for accelerators, *uncorrelated* background for the larger amplitude ground movements correlated in time and space. The latter are present in the spectra (power spectral density) as several well marked peaks corresponding to the upper crust noises at l-4 Hz, microseismic waves at 0.07-0.16 Hz, tidal waves with periods of subharmonics of 24 hours (see e.g. [1, 4, 5, 6, 7, 8, 9]). There are also an ambient low-frequency ground motion generated by local sources such as wind, air pressure variation, temperature gradients, ground water, precipitation, etc., which can't be adequately treated as waves propagated in the ground (see e.g. [2, 10, 11]). Nevertheless, this ground motion is regular - it does not take place in the absence of the origin (wind, temperature fluctuations, etc.). Conversely, the *ATL* diffusion seems to be an inevitable process.

The power spectrum density (PSD)[1] of the diffusive motion in the frequency domain is equal to [12, 13]:

$$S_{ATL}(f) = \frac{AL}{2\pi^2 f^2}, \quad f > 0, \tag{2}$$

and in the wavenumber $k = 2\pi/\lambda$ domain:

$$S_{ATL}(k) = \frac{2AT}{k^2}, \quad k > 0, \tag{3}$$

This article presents an overview of the ground diffusion, the experimental methods used for its detection, and its impact on beams in accelerators. Although most of the examples discussed in the paper can be found elsewhere, several results are either quite new or were not correctly published. These are the processing of data from Esashi Earth tide station, on LEP alignment in 1992-1994, on sea level variations at Japan coast since 1930. Based on numerous results, we discuss the limits of validity of the *ATL* law and make estimation of the orbit diffusion in future accelerator facilities.

1.2 Accelerators

Before starting the review, let us briefly describe why we are concerned about the impact of diffusion on accelerators.

In an ideal accelerator with well-aligned magnetic elements, the closed orbit passes through the centers of bending magnets and quadrupoles to provide optimal conditions for the operation of the machine. Any alignment errors cause a closed orbit distortion (COD) in circular machines or a trajectory distortion in linear colliders (LC), reduce the

[1] The power spectral density is defined as the variance of the process in a unit frequency band; thus, mean the square value of the process *x(t)* in the frequency band from f_1 to f_2 can be obtained from its spectrum $S_x(f)$ as:

$$\left\langle x^2 \right\rangle [f_2 > f > f_1] = \int_{f_1}^{f_2} S_x(f) df.$$

dynamic aperture of the ring, and, in an extreme situation, make it impossible to run the machine.

Typically, a correction system is used to counteract the magnetic errors that build up and accumulate during the operation of the machine. In large accelerators, such as the Superconducting Super Collider (SSC) (- unluckily terminated in 1993), the Large Hadron Collider (LHC), HERA, and future Linear Colliders, which have many hundreds of magnetic elements, one of the most important sources of magnetic errors on a long time scale is the ground motion that displaces the magnets from their original position.

Slow ground motion with frequencies much less than the characteristic frequencies of an accelerator (i.e. revolution frequency, or repetition frequency in LC) usually has been considered as not seriously affecting machine operation because complete space and time coherence of the magnet displacements has been assumed. we will consider, as a real example, "microseismic waves" caused by ocean waves at the closest coasts. They have a period of approximately 7 seconds and a wavelength $\lambda \approx$ 20 kilometers, their amplitudes are about 0.1-10 μm. Experimentally it has been proved that there is good temporal correlation up to 200 s [1] an spatial correlation up to 3000 m [6]. The betatron wavelength λ_β which is of the order of hundred(s) meters in large accelerators (some dozens meters in LCs), is much less than λ. These ground waves perturb the beam motion only adiabatically, the orbit response being proportional to a factor of $(\lambda_\beta/\lambda)^2$ [14] which is about $10^{-3} \div 10^{-6}$, and therefore the influence is practically negligible. The response is significant if the wavelength is comparable or less than the betatron wavelength. In other words, the most severe source of orbit distortion is not fully correlated relative motion of neighboring focusing magnets along the beam path - exactly what the *ATL* law is (1) for.

An equation for rms closed orbit distortion Δx_{COD} caused by random (though without any assumptions on spatial correlation) quadrupole displacements in a large circular accelerator was derived in Ref.[15]:

$$\langle \Delta x_{COD}^2 \rangle = \frac{\beta N}{64 F_0^2 \sin^2 \pi\nu} \left(k_{[\nu]} (\sqrt{\beta_F} - \sqrt{\beta_D})^2 + k_{N/2-[\nu]} (\sqrt{\beta_F} + \sqrt{\beta_D})^2 \right) \qquad (4)$$

here N is the total number of quadrupoles in symmetrical *FODO* lattice of the ring, F_0 is the focal length of each quadrupole, ν is the tune of the machine, $[\nu]$ is the integer part of the tune $\beta, \beta_{F,D}$ are the values of beta-function at the point of observation and in the positions of the focusing and defocusing lenses. k_m are the coefficients of the Fourier transformation of the correlation function of magnets displacements $K(i-j) = \langle \delta_i \delta_j \rangle$:

$$k_m = 2 \sum_{i=0}^{N-1} K(i) \cos\left(\frac{2\pi i m}{N}\right), \quad for \quad 0 < m < N/2,$$

$$k_0 = \sum_{i=0}^{N-1} K(i), \quad k_{N/2} = \sum_{i=0}^{N-1} (-1)^{-i} K(i). \qquad (5)$$

Two noise harmonics give the largest contribution - the result, similar to the one in the case of plane waves [14].

For fully uncorrelated quad displacements with rms value δ formula (4) gives :

$$\langle \Delta x^2_{COD} \rangle = \frac{\beta N < \delta^2 >}{16 F_0^2 \sin^2 \pi\nu} (\beta_F + \beta_D) \tag{6}$$

In the case when the quadrupoles movements are governed by the *ATL* law, the orbit variance was found in [15]:

$$\langle \Delta x^2_{COD} \rangle = \frac{\beta ATC(\beta_F + \beta_D)}{8 F_0^2 \sin^2 (\pi\nu)} \tag{7}$$

For practical applications, the mean (over the circumference and averaged in time) square COD could be derived assuming $\sin^2(\pi\nu) \sim 0.5$ and *FODO* focusing structure with 90 degrees betatron phase advance per cell:

$$\langle \Delta x^2_{COD} \rangle \simeq 4ATC \tag{8}$$

Thus, larger orbit drifts are expected at large accelerators. Approximate formula can be derived for the mean square beam-beam displacement at the interaction point (IP) of LC caused by linac focusing magnet movements:

$$\langle \Delta x^2_{IP} \rangle \simeq 32\pi AT\beta^*\nu \tag{9}$$

where ν is number of betatron oscillations along a linac, β^* is the beta-function at the IP.

2 Diffusion in Time and Space Domain: How Does It Look Like ?

In this section we consider several recently observed manifestations of the diffusion in space and time domains, and at accelerators.

2.1 Diffusion in Time - Esashi Earth Tide Station (Japan)

The Esashi Earth tide station is situated in the North-West of Japan. It occupies a tunnel in granite mountain side. Two 50-m long water levels directed to South-North and East-West are at about 160 m from the tunnel entrance and about 60 m under the mountain surface. These tiltmeters detect vertical elevation difference. Observations started in June 1979 by National Astronomical Observatory Mizusawa were continued since November 1993 in collaboration with S.Takeda group of KEK. Fig.1 presents almost 15-years-long monthly record of S-N and E-W tilts [16].

We have extracted linear trends from these data and performed calculation of the mean value of the first difference squared, i.e. $dH^2 = < (\theta(t+T) - \theta(t))^2 >$. It yields the dependence of the variance versus time interval T as presented in Figs.2 a),b) which can be approximated by the least square linear fit with coefficient of $0.015 \pm 0.0025 [\mu rad^2/month]$ for E-W tilt and of $0.019 \pm 0.003 [\mu rad^2/month]$ for S-N tilt (see dashed lines in Fig.2). Error bars represent $\pm 2\sigma$ statistics which lacks at time intervals of more than 3 years. Conversely, there is large statistics for $T < 10$ months, the errors are small and $dH^2(T)$ is pretty linear function.

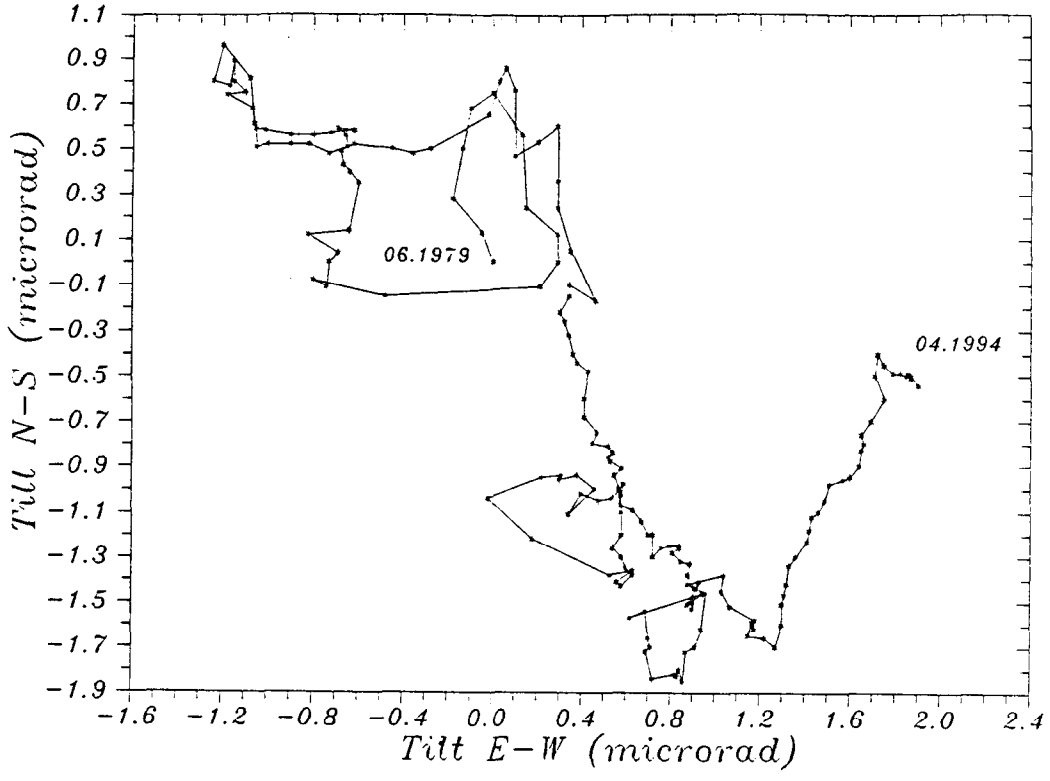

Fig.1 Secular tilting motion at Esashi station in 1979-1994 (data taken from [16]).

The observed dependence of the variance as $\propto T$ is characteristics of a random walk (or Brownian) process. As we assume validity of the *ATL* law, the diffusion coefficient is estimated as $A = L \times dH^2(T)/T \simeq (0.33 \pm 0.05).\ 10^{-6}\,\mu m^2/(s \cdot m)$.

2.2 Diffusion in Space - CERN LEP Tunnel Motion

Several times a year, measurement of more than 700 quadrupole positions and realignment procedure are performed at LEP(CERN) over a circumference of 26.6 km. The LEP magnets elevation in 1993-1994 [17] are presented in Fig.3. As the median plane of LEP is some μrad tilted, the mean tilt was subtracted from the raw data. Left top drawing of Fig.3 shows vertical quads positions of LEP quads in April 30, 1993, just after making the alignment to a smooth curve. At that time roughness of the curve is assumed to be mostly due to instrumentation accuracy. Left bottom picture shows measured positions at January 28, 1994, i.e. almost 9 months after the 1993 alignment. One can see that the

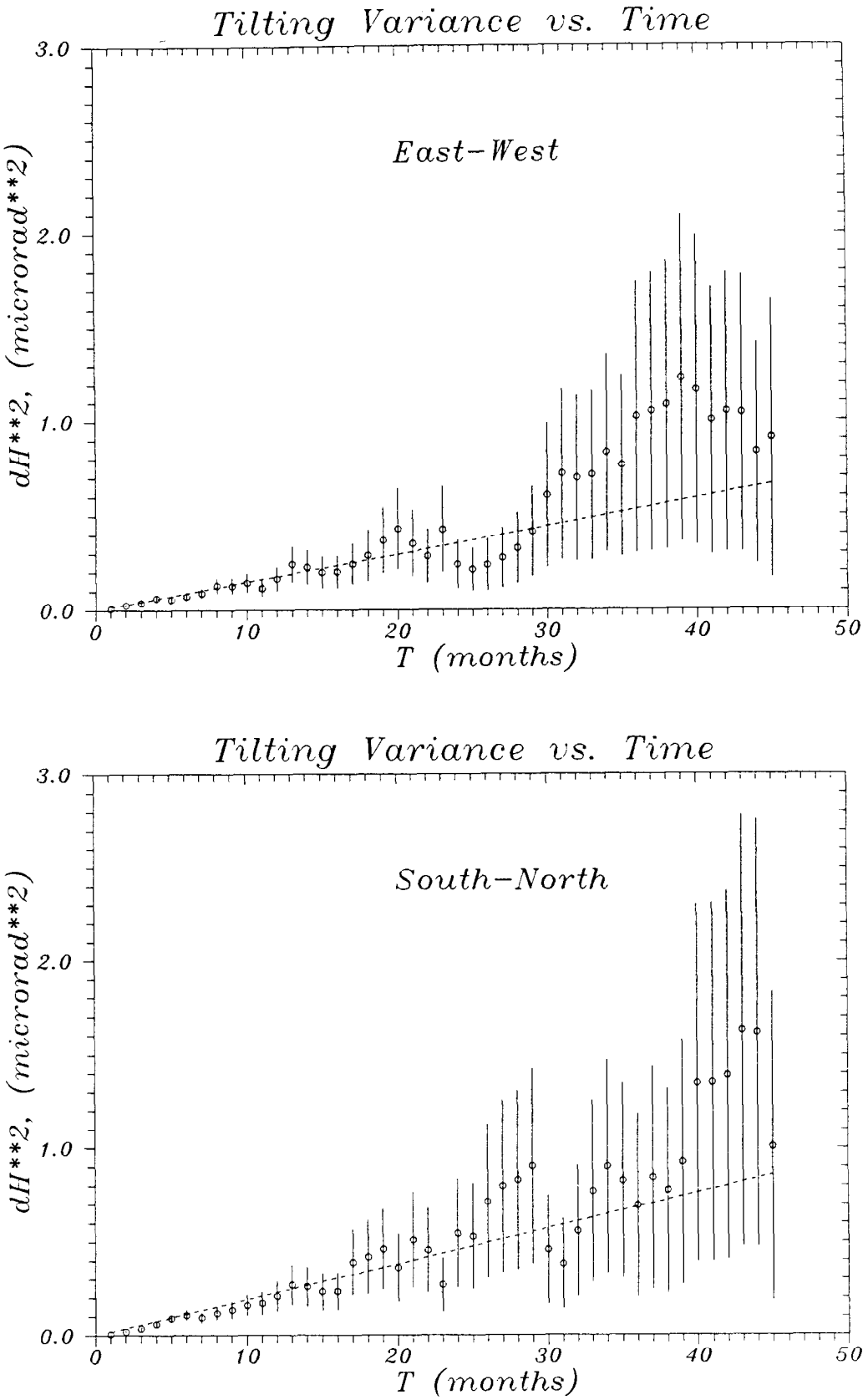

Fig.2 Variance of the first difference vs. time interval:
a) (upper plot) for Esashi East-West tiltmeter,
b) (lower plot) for Esashi South-North tiltmeter.

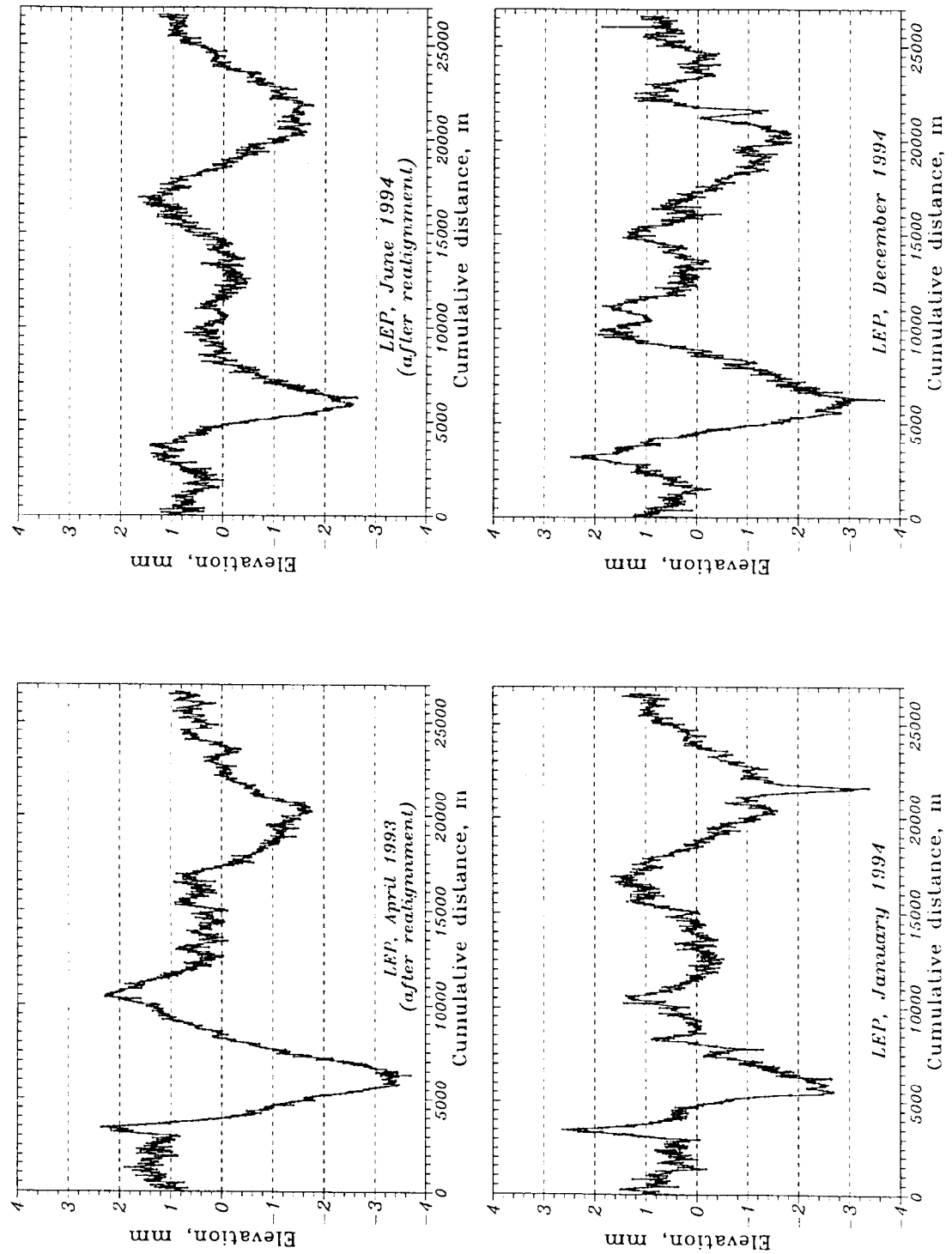

Fig.3 LEP elevations in 1993–1994 (from Ref.[17]).

line is more rough and several obvious peaks have appeared, the biggest are around 3500 m and 21500 m. Then, the realignment had been done and the LEP magnets elevations at June 6, 1994 are presented in right top figure. Major peaks are obviously smoothed, but 6 month after, in December 1994, they are seen again, as well as other less significant changes are recognizable (see right bottom plot).

Further data processing made by the author, includes: 1) 1 km pieces of the LEP circumference around 3500 m and 21500 m were excluded out of further consideration, as these are regions of well known geological instability; 2) mean value of each quadrupole elevation was calculated from elevations of its' ends; 3) as we're not interested in smooth spatial curves, the lowest five Fourier harmonics were subtracted from the data.

After all, the variance of the first difference was calculated as

$$dH^2(L) = < (H(l+L) - H(l))^2 > . \qquad (10)$$

where H(Z) is the vertical coordinate of the quad positioned at the point *l*, and brackets < . . . > denote averaging over all possible pairs of quads distanced by *L*.

The results are shown in Fig.4. The χ^2 criteria gives following linear approximation (*L* in meters, dH^2 in mm^2):

$$\begin{aligned}
&30.04.1993 \quad dH_I^2(L) \approx \quad 0.00016 \cdot L \quad + 0.015 \\
&28.01.1994 \quad dH_{II}^2(L) \approx \quad 0.00037 \cdot L \quad + 0.022 \\
&06.06.1994 \quad dH_{III}^2(L) \approx \quad 0.00024 \cdot L \quad + 0.001 \\
&\text{Dec.}1994 \quad dH_{IV}^2(L) \approx \quad 0.00034 \cdot L \quad + 0.017
\end{aligned}$$

We see that for $L < 1000$m the variances of aligned accelerator are $1.5 \div 2$ times less than several months after the alignment procedures. It means that the realignment really reduces roughness of elevation, although it better smooths large peaks due to strong geological drifts.

Implying, that the variances dH_I^2 and dH_{III}^2 are mostly due to instrumentation noise, the rms error of the LEP levelling process can be estimated as $0.4 \div 0.5 \mathrm{mm/km^{1/2}}$.

The excess of the variance over the instrumentation noise level should be assigned to the ground diffusion. Again, assuming validity of the *ATL* law, we get two estimates of the diffusion constant *A:*

$$A_{II-I} = \frac{dH_{II}^2(L) - dH_I^2(L)}{L \cdot 9\ months} \simeq 0.9 \cdot 10^{-5}\ \mu m^2/(s \cdot m), \qquad (11)$$

and

$$A_{IV-III} = \frac{dH_{IV}^2(L) - dH_{III}^2(L)}{L \cdot 6\ months} \simeq 0.7 \cdot 10^{-5}\ \mu m^2/(s \cdot m), \qquad (12)$$

which are closely related.

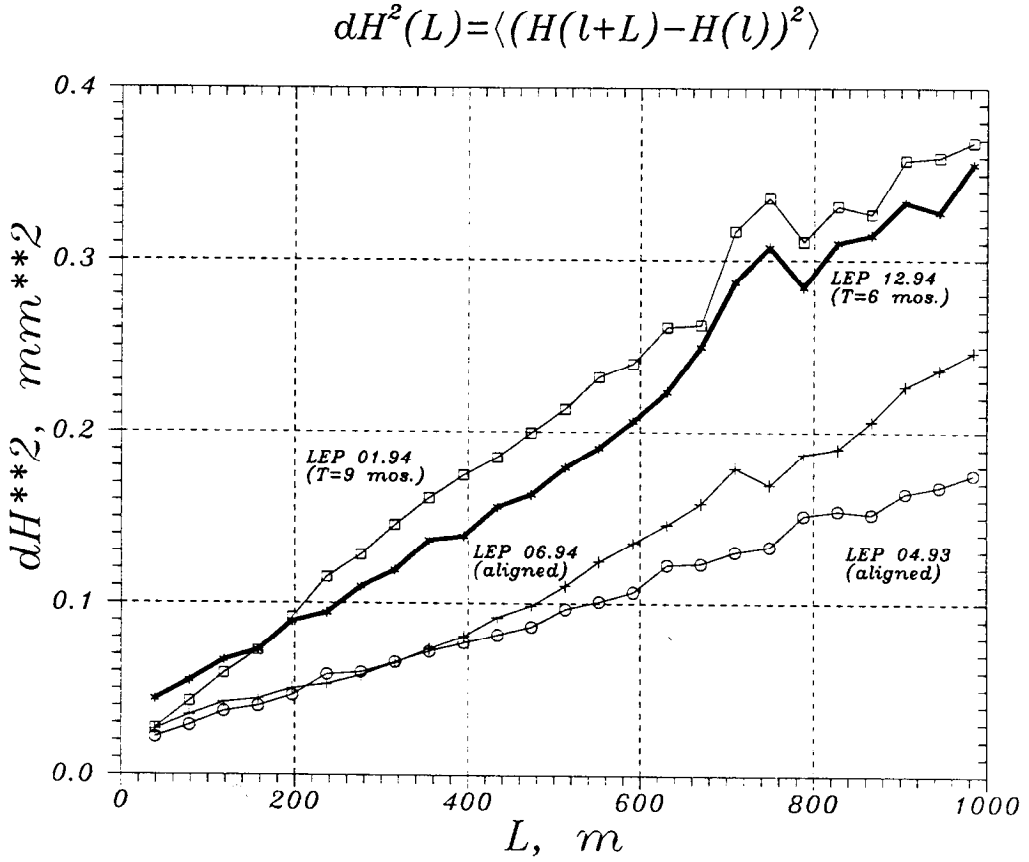

Fig.4 Mean squared height difference vs. *L:*
04.1993 - LEP is aligned, 01.1994 - 9 months after;
06.1994 - LEP is aligned, 12.1994 - 6 months after.

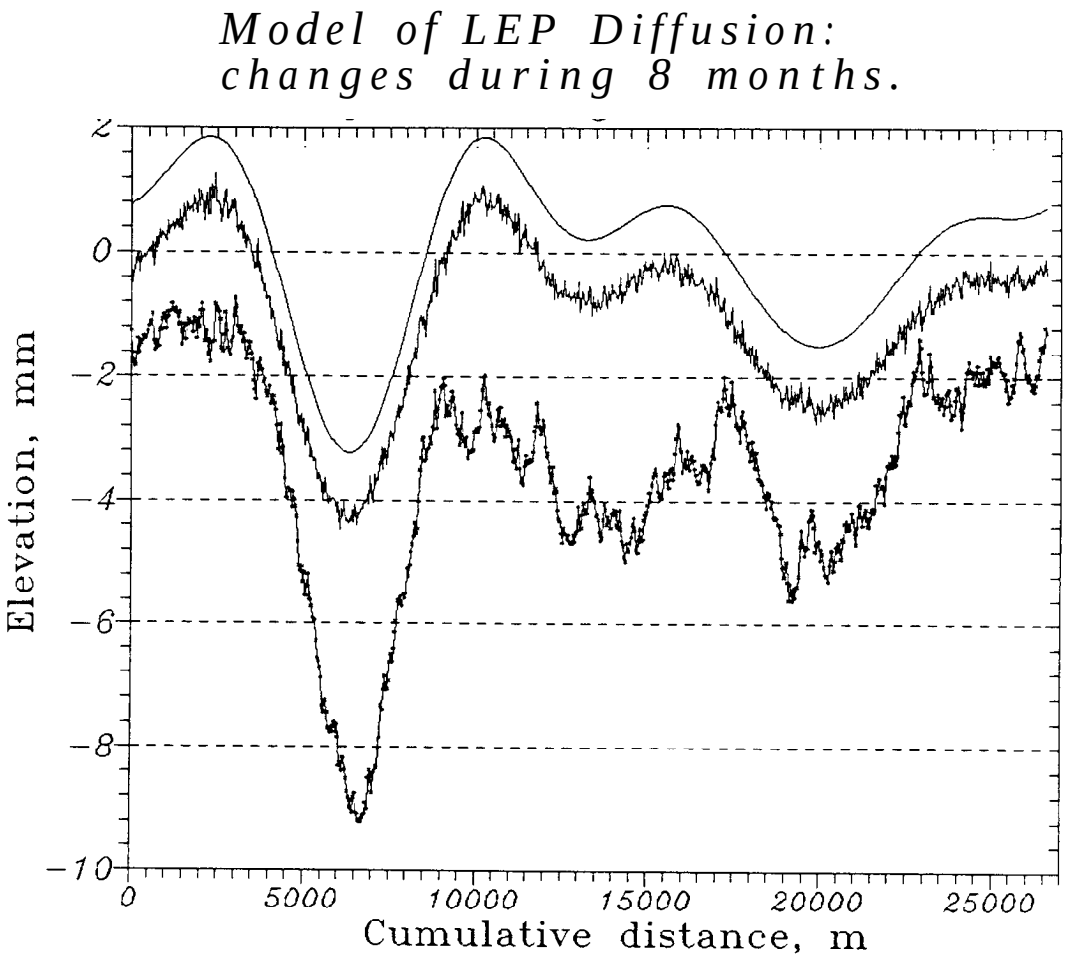

Fig.5 Three models of the LEP quad positions [20]:
upper - aligned to smooth curve, middle - with random displacements, lower - in accordance with the ATL law.

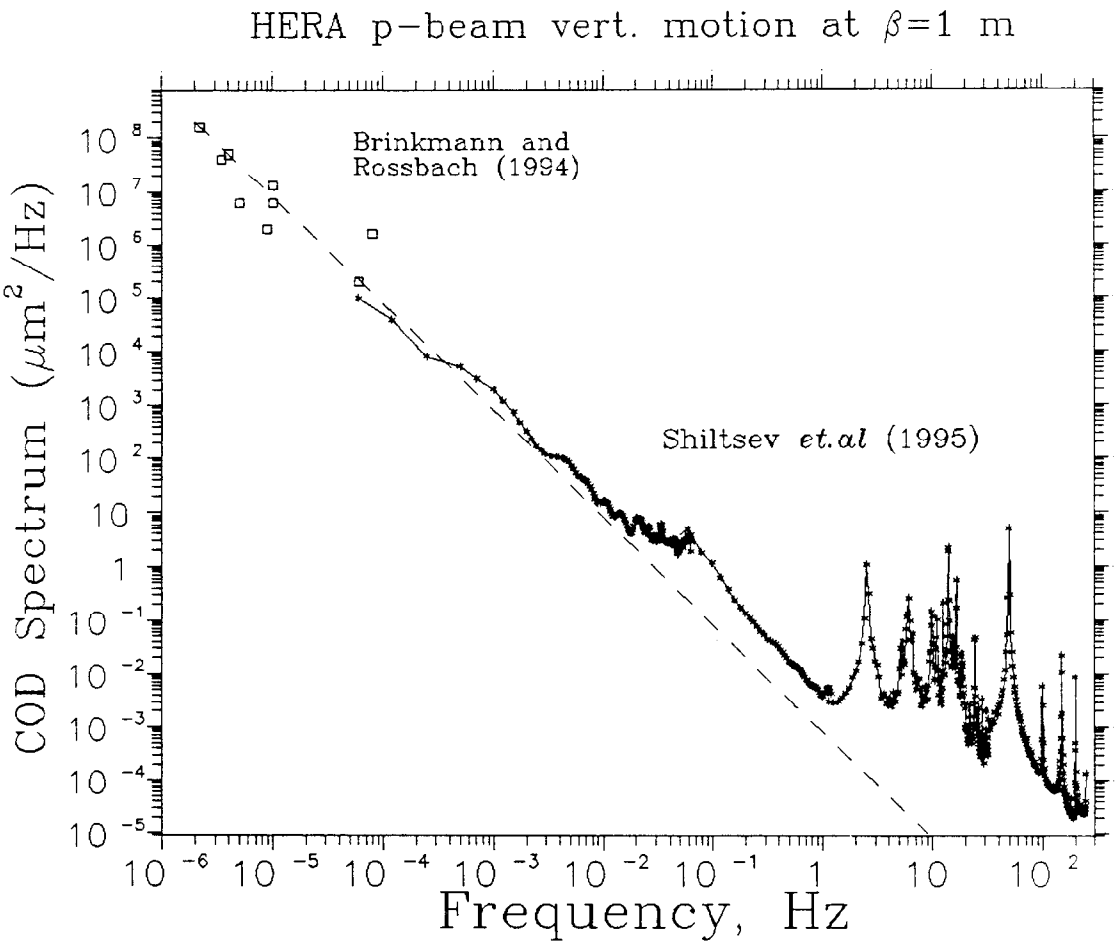

Fig. 6 PSD of HERA proton orbit vertical motion normalized to β =1 m. Dashed line is for the *ATL* expectation (from Ref.[18, 9]).

Therefore, the LEP alignment data demonstrate that the bigger the distance between tunnel pieces, the larger variance of their relative displacement in time.

Fig.5 demonstrates the peculiarities of the ground diffusion. Three models of the LEP magnet elevation are shown (for the sake of presentation they are vertically displaced): the upper is for an "ideal" alignment; in the middle plot, some random uncorrelated displacements are added; the lowest line presents modeling in accordance to the *ATL* law. Qualitative difference is seen between the random errors line and the *ATL* line.

2.3 Beam Orbit Diffusion - HERA *e - p* Collider

To a greater or lesser extent long-term orbit drifts are seen at all accelerators and machine operators or/and automatic correction systems counteract it. As large colliding beam facilities are particularly sensitive to the orbit motion, some extended investigations of the issue have been carried out there. As an example, we discuss recent studies at the HERA electron-proton collider at DESY in Hamburg.

The power spectral density of the HERA proton beam vertical orbit (scaled for beta function β =l m) is shown in Fig.6. Continuous line represents the Fourier spectrum of readings from one specific beam position monitor (BPM) in HERA-p [9]. Peaks above 2 Hz reflects technological equipment noises. As continuous observations were performed repetitively within several hours of the proton beam lifetime, the lowest frequency of this spectrum is about $5{\cdot}10^{-4}$ Hz.

The squares at lower frequencies represent the Fourier spectra of proton orbit, from different fills of the storage ring [18]. The procedure was to measure the closed orbit position at all 131 BPMs in HERA-p. If the result is subtracted from a previous one, a so-called difference orbit is obtained, indicating any eventual orbit drift. The analysis of difference orbits was limited to time intervals during which no intentional change of the closed orbit occurred (about 5 days maximum).

The dashed line in Fig.6 shows the PSD scaling as expected by the *ATL* rule:

$$S_{COD}(f) = \frac{8 \cdot 10^{-4}}{f^2} \quad [\mu m^2/Hz]. \tag{13}$$

Within a factor of 5 this line acceptably fits to the experimental spectrum from $2{\cdot}10^{-6}$ Hz up to almost 1 Hz. In time domain such PSD corresponds to irregular noisy proton orbit difference drifts - like "random walk" - with rms magnitude growing as cx $\sqrt{T}$ for time intervals *T* from some seconds to some days.

Long term drifts of dipole corrector currents and temperature drifts were estimated to be negligible. Low-frequency noises of BPMs also could not lead to the measured drifts, because uncorrelated drifts of different monitors can not perform orbit oscillations along the ring with betatron frequency that was observed in fact. Thus, the motion of quads seems to be the only candidate that can explain HERA orbit drifts and one can estimate the diffusion coefficient:

$$A_p = (1.5 \pm 1.0) \cdot 10^{-5} \quad [\mu m^2/(s \cdot m)] \tag{14}$$

- here we used combination of Eq.(2) and Eq.(7) and the HERA-p parameters ν_y=33.298,

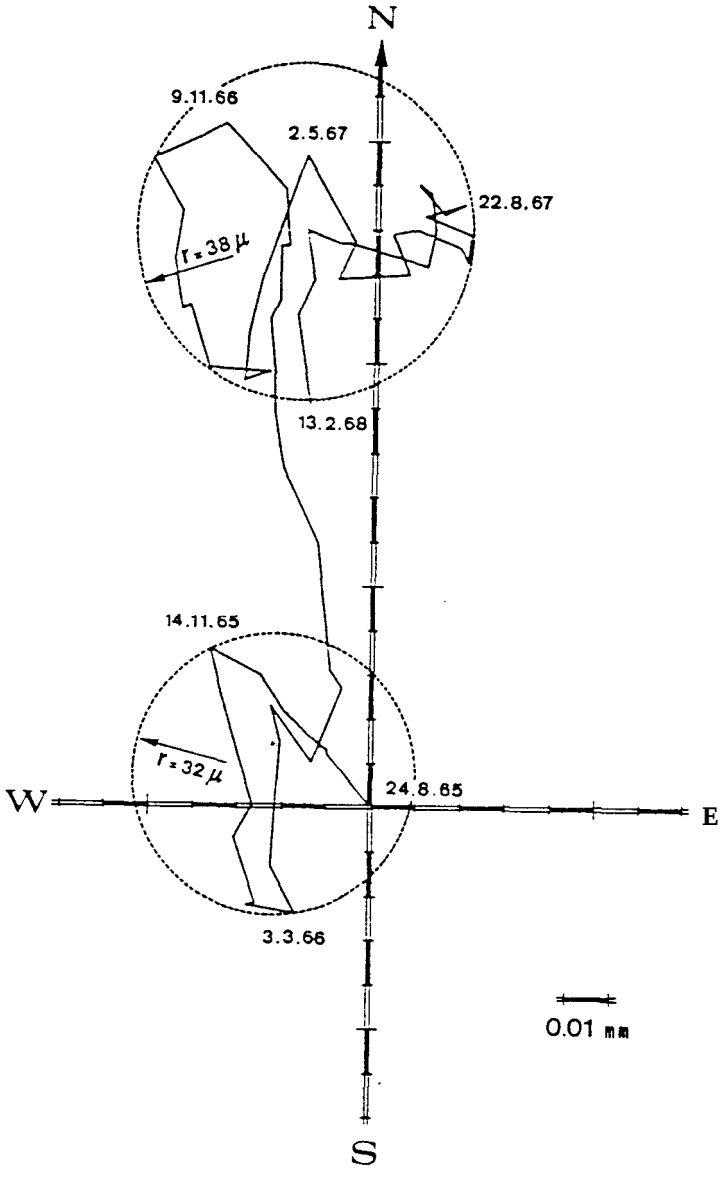

Fig.7 Horizontal movement of the PS central pillar in 1965 - 1968 (from Ref.[19]).

β_D = 13.8 m, β_F=80.4 m, F =16.8 m, C =6336 m. Sign "±" in (14) refers to wide spread of the constant rather than statistical error.

It was stressed in Ref.[18], that having completely different magnet lattice, the HERA electron ring orbit also performs diffusion with the constant $A_e \simeq$ (0.4±0.1). $10^{-5} \mu m^2/(s \cdot$ m) which is applicable up to l-month-long time intervals.

3 Overview of Diffusion Measurements

Below we briefly consider several previously observed manifestations of the ground diffusion.

3.1 Inverted Pendulum at CERN

Possibly the first manifestation of the ground diffusion at accelerators was detected in movement of central CERN Proton Synchrotron (PS) pillar over more than 2 years - see Fig.7 from Ref.[19]. From 24.08.1965 to 13.02.1968 a pair of horizontal pendulums were mounted on the PS anchored in the molasses 10 m below ground level. These instruments measure the variations of their support in relation to the direction of the vertical, and, therefore, the movement of the vertical axis of the 10 m pillar. Such an inverted pendulum performed irregular motion that looks like Brownian motion. Extracting some linear trend (well remarkable in South-North direction), one can find, that in both directions the variance grows about linearly in time, and the coefficients of the *ATL* diffusion are equal to (0.2 ± 0.4) $\cdot 10^{-5} [\mu m^2/($ s $\cdot$ m)] (these values correspond to the variances $\Delta x^2 \simeq \Delta y^2$ of about $500 \div 900 \mu m^2 \approx (22 \div 30\ \mu m)^2$ at time interval of T =9 months and L = 10 m) [20].

3.2 Laser Interferometry Measurement

Article of F.Wyatt [11] describes measurements of horizontal motion of massive near surface monuments at Pinon Flat Observatory, California. The monuments were emplaced in competent, weathered granite. Several different techniques were used to detect the monument movements, including tiltmeters and laser interferometers. The last one was implemented in so-called "optical anchor", which measured the difference in length of two optical paths in two some 26 m long boreholes inclined at 30 degrees to the vertical. Optical retroreflectors were mounted near the bottoms of these holes at the depth of about 24 m. An Michelson interferometer was utilize to determine the path difference and, therefore, motion of the surface with respect to bedrock.

1974-1980 observations have shown abnormally small horizontal displacements of the order of 50 μ per year, demonstrated influence of seasonal temperature variations and precipitation. Power spectral density of the surface horizontal displacements is presented in Fig.8 [11]. The dashed line in Fig.8 made by me presents satisfactory fit of the optical anchor data up to 1 year time interval:

$$S_{PFO}(f) = \frac{1.2 \cdot 10^{-7}\ [\mu m^2 \cdot Hz]}{f^2}. \qquad (15)$$

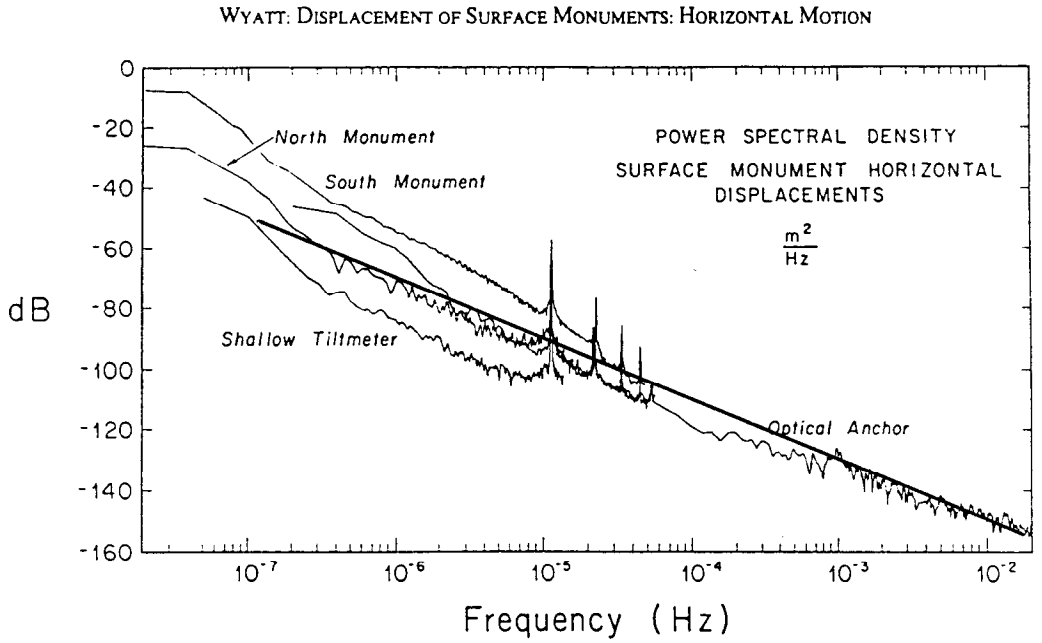

Fig.8 Power spectral density of the near-surface horizontal displacements at Pinon Flat observatory [11]. Straight line indicates the ATL law scaling.

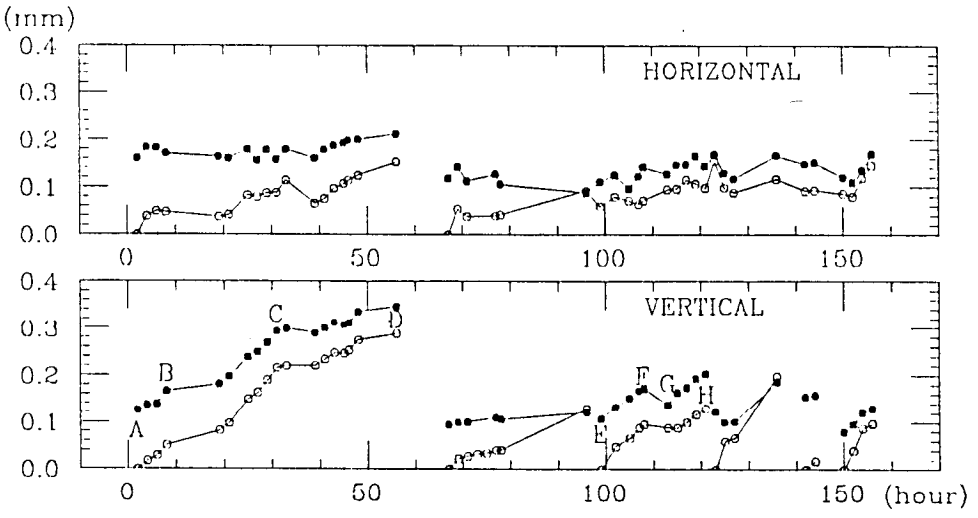

Fig.9 Changes of COD in TRISTAN ring (from Ref. [21]). a) - 3 years (1985-1988), b) - 3 years (1988-1991), c) - 6 years (1985-1991), d) - 12 years (1976-1988).

Table 1: Develonment of TRISTAN COD between corrections

Time interval (h)	$\sigma_2\,(\mu m)$	T (h)	$A = \frac{\sigma_2^2}{4TC}$ $(\mu m^2/(s \cdot m))$
O-50	300	50	$0.5 \cdot 10^{-4}$
66-96	140	30	$0.15 \cdot 10^{-4}$
97-121	140	24	$0.19 \cdot 10^{-4}$
123-135	220	12	$0.9 \cdot 10^{-4}$
150-158	120	8	$0.4 \cdot 10^{-4}$

Taking L = 24 m one obtains with use of Eq.(2) the value of the diffusion constant:

$$A_{PFO} \simeq 1.0 \cdot 10^{-7} \quad [\mu m^2/(s \cdot m)], \tag{16}$$

that is small in comparison with previous results.

3.3 Electron Beam Orbit Drifts in TRISTAN Ring

Some early data on long term orbit drifts (corresponding to a time period of a few days) have been reported from the KEK TRISTAN storage ring. Figure 9, taken from Ref.[21], shows closed orbit distortions (COD) in TRISTAN storage ring at the energy of 8.0 GeV. Full circles in the figure are the rms values of COD σ_1 as a function of time calculated with the use of the formula $\sigma_1^2 = N^{-1}\sum_{i=1}^{N} x_i^2$, where x_i is the measured displacement of the COD relative to the "ideal" orbit at the location of the i-th BPM and N = 392 is the total number of BPMs. Open circles represent the value of $\sigma_2, \sigma_2^2 = N^{-1}\sum_{i=1}^{N}(x_i - x_{i0})^2$, where x_{i0} is the initial value of x_i during an operation cycle between two successive corrections of the orbit. Note that the horizontal COD is smaller than the vertical one. It has been observed that when σ_1 reached values larger than 100 - 200 μm, the maximum beam current degraded significantly so that a correction of the orbit was needed toward the "ideal" one (sharp drops at points D, E, H, and some others in Figure 9). Using the data in Figure 9, we'd analyzed in [15] how CODs have been developing between the corrections. The results are summarized in Table 1, where the first column shows the time span in Figure 9, T is the duration of the time interval between the corrections of the orbit, and σ_2 is the COD accumulated in this time. We have also calculated the parameter $A = 0.25\sigma_2^2 \cdot T^{-1} \cdot C^{-1}$ (C = 3000 m is the TRISTAN circumference), that accordingly to Eq.(7) gives the upper estimate of diffusion parameter due to ground motion.

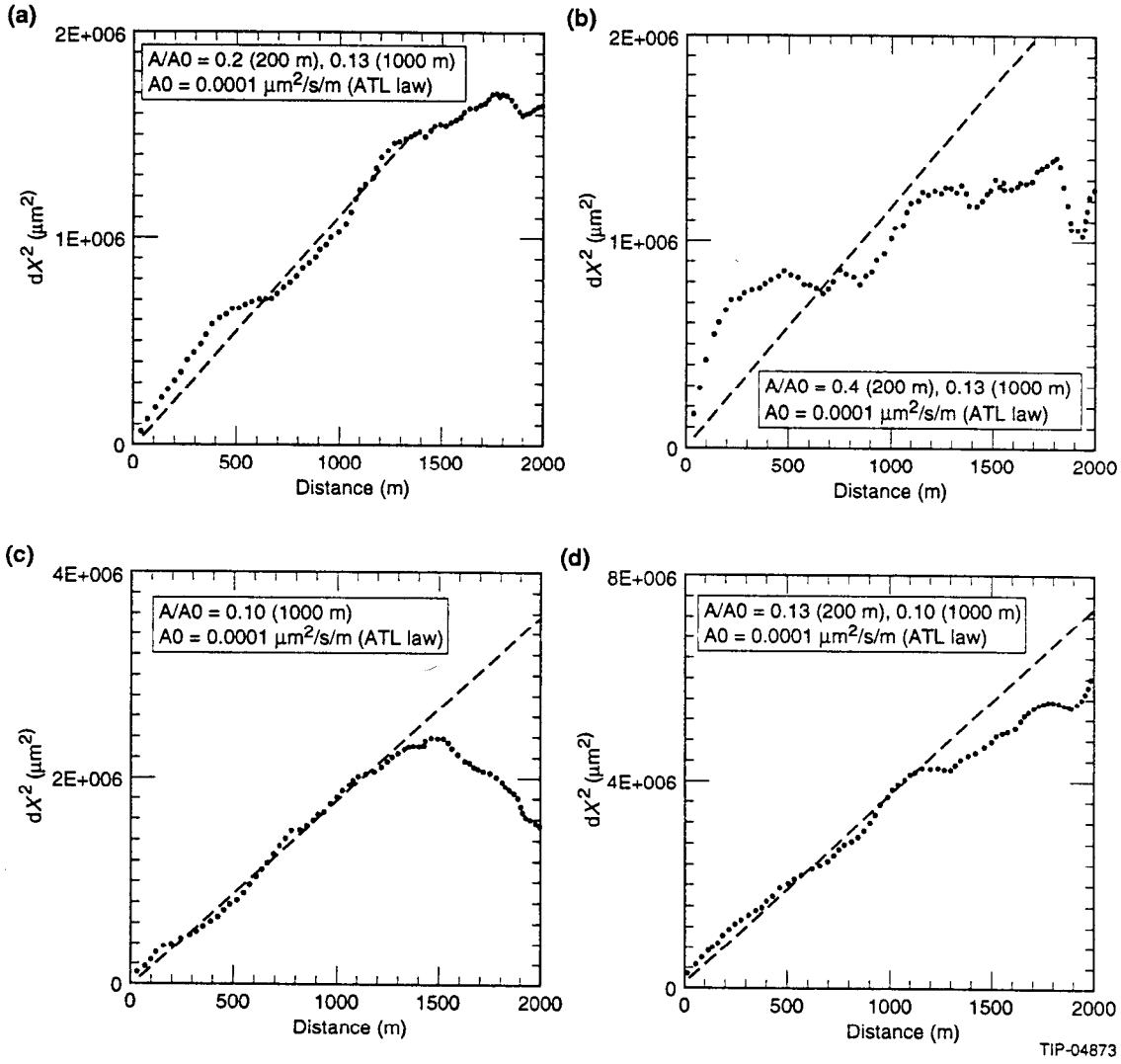

Fig.10 The variance of relative displacement of the SPS quadrupoles during different time periods vs. *L:* a) - 3 years (1985~1988), b) - 3 years (1988-1991), c) - 6 years (1985-1991), d) - 12 years (1976-1988). Figure taken from Ref.[12].

From Table 1 one can derive $A_{TRISTAN}$ = (4.3 ± 3.0). $10^{-5}\mu m^2/(s\cdot m)$, which is quite consistent with the coefficient found from the HERA orbit drifts (see above).

3.4 Accelerator Alignment Data: SPS, SLC, PEP, UNK

Numerous data on alignment and realignment at existing accelerator facilities can be found in recent publications, however, we restrict ourself with consideration of several machines where some analysis of primary data was done.

CERN Super Proton Synchrotron 1976-1991 The SPS is an alternated gradient synchrotron constructed at CERN in mid-1970s. It consists of about 744 dipoles and N=216 quadrupoles placed practically uniformly over the ring, with a mean radius *R* = 1100 m. Primary data from an optical survey were provided by J.-P.Quesnel of CERN and processed in Ref.[12] by the procedure similar as in the *LEP* Alignment section above. Resulted variances of the relative vertical displacements of the quads versus distance *L* are presented in Fig.10 from [12]. Fig.10) shows $< d X^2(L) > = < (X(l+L)-X(l))^2 >$ for the quads displacement occurred from 1985 until 1988 - i.e. X = $x_{1988} - x_{1985}$, and linear fit gives $A = 1.3\cdot 10^{-5}\mu m^2/(s\cdot m)$. Corresponding diffusion constants for 1988-1991, 1985-1991, and 1976-1988 movements are (1.3,1.0,1.0) $\cdot 10^{-5}\mu m^2/(s\cdot m)$ respectively - see Figs. 10 b),c),d) - that results in the mean value of about A_{SPS} = 1.1 $\cdot 10^{-5}\mu m^2/(s\cdot m)$. Please, denote that time intervals vary from 3 years to 12 years, nevertheless the diffusive constants are almost the same. Therefore, the SPS observations can be considered as a demonstration of the *ATL* diffusion in both space and time domain.

UNK Site, SLAC Linac Tunnel, PEP Tunnel Originally in Ref. [1], it was found that Eq.(1) with the factor A_{UNK} = 1.0 $\cdot 10^{-4}\mu m^2/(s\,.\,m)$ is in good agreement with the data obtained from theodolite measurements of movements of few dozen surface monuments along 2 km long straight line at the UNK collider construction site (Protvino) for *T* about 2 yr. Also, analysis performed in Ref.[3] showed that Es.(1) is consistent with observation of SLAC Linac (SLC) tunnel ($L \simeq 3$ km) displacements during 17 years (primary data were taken from [4]), and SLAC PEP tunnel displacements during 20 months (1989-1991) over the circumference of 2000 m (primary data were taken from [22]). We'd like to note that SLC data were obtained with the use of a laser alignment system, while *"circumferentially continuous"* water level is implemented for the vertical alignment of the PEP.

Fig.11 from [1a] presents the relative displacement variances versus distance for SPS, UNK, SLC and PEP accelerators; dashed line shows the *ATL* law scaling with *A* = $10^{-4}\ \mu m^2/(s\cdot m)$.

The tunnels in SLAC sit on or are mined in grey unweathered well cemented tertiary myocene sandstone. Possibly due to "*cut and* cover" construction and smaller depth, the SLAC linac tunnel demonstrates faster diffusion than the PEP tunnel - the coefficients are $A_{SLC} = (2\pm 1)\cdot 10^{-4}\mu m^2/(s\cdot m)$ and $A_{PEP} = (1\pm 0.5)\cdot 10^{-4}\mu m^2/(s\cdot m)$ correspondingly.

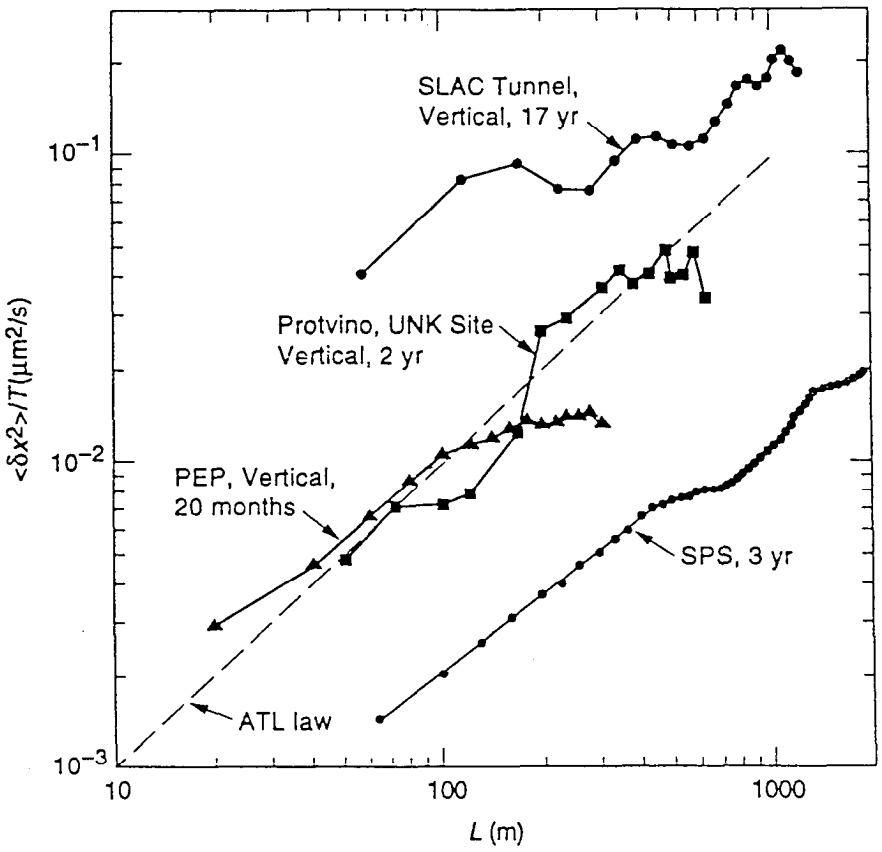

Fig. 11 The variance of relative displacements divided by time of observations vs. distance between points for SPS, PEP, UNM, SLC (data taken from Ref.[15]).

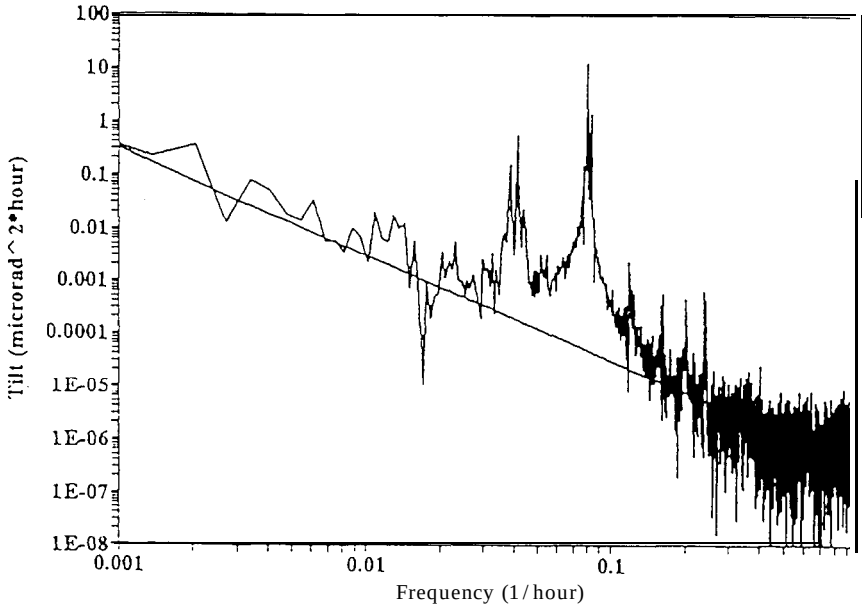

Fig.12 Aspectrum of ground motion. A straight line indicates $1/f^2$

3.5 Hydrostatic Levels Measurements in Japan

Precise measurements with hydrostatic level system were performed in 1992-1994 by the group of Prof. Shigeru Takeda of KEK. In the longest, L =50 m variant, the system was used in in Sazare mine in 1992-1993 [8]. The mine is about 300 m under the surface of hard rock (green schist) mountain slope. The water tube tiltmeter with an overall accuracy of 0.1 μm have shown that the tilt is a superposition diffusive drifts, tides and precipitation effects. The PSD of the tilt observations up to 100 hours is shown in Fig.12 from [8]. One can clearly see several tidal peaks in the spectrum. Ta straight line corresponds to the *ATL* law spectrum (2) with $A = 0.8 \cdot 10^{-7} \mu m^2/(s \cdot m)$. Authors also revealed valuable seasonal variation of the diffusive constant: from maximum 1.5 $\cdot 10^{-7} \mu m^2/(s \cdot m)$ in December 1992 down to minimum 0.1 $\cdot 10^{-7} \mu m^2/(s \cdot m)$ in March 1993.

Similar investigations were carried out in the base of TRISTAN storage ring [5] and there were found that power spectral densities could be also approximated by Eq.(2) with considerably bigger value of the diffusion coefficient: $\simeq 0.5 \cdot 10^{-5} \mu m^2/(s \cdot m)$ found for few days observation with L = 42.5 m long tiltmeter; and $\simeq 0.4 \cdot 10^{-6} \mu m^2/(s \cdot m)$ for 12.5 m long tiltmeter.

3.6 Measurement With Straight Wire

Tight metallic (invar or tungsten) wires are widely used for alignment purposes. For example, results of measurements with up to 20 m long wire can be found in [1, 2]. Fig.12b shows power spectral density of relative movements of two 5 m long girders - detected with the use of the wire (circle) - in comparison with girder's absolute motion measured by a seismometer (stars). One can see that below 1 Hz the absolute movement is much bigger than the relative displacement. The later can be roughly approximated by Eq.(2) with A = (1 ± 0.5) $\cdot 10^{-4} \mu m^2/(s \, . \, m)$.

4 Discussion

4.1 What is Relevant for the Diffusion ?

Table 2 summarize all the data on ground diffusion and presents the coefficient A, time interval T and spatial interval L where the diffusion took place (for beam orbit data L was taken to be about *FODO* cell length), plane (V is for vertical, H is for horizontal) and effective depth of observations.

The plot of *A's* versus the depth (see Fig.13) shows that in spite of enormous spread of results there is a general tendency to smaller A at bigger depth H. Fit accordingly to *Fractal Model of Ground [3]* gives a $1/H^{3/4}$ scaling presented by dashed line in Fig.13.

Valuable deviations of the data from the fit possibly emphasize an importance of site dependent parameters, the most influential possibly are the type of the rock and climate.

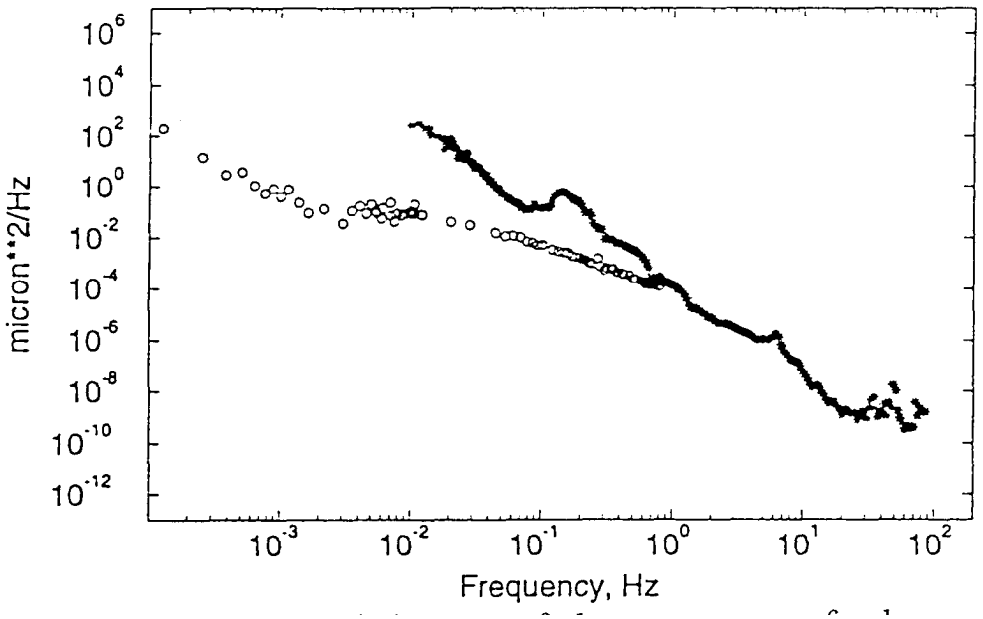

Fig.12b: Power spectral density of the spectrum of relative movements of two 5 m long girders (circles) in comparison with the PSD of absolute ground motion (stars) (from Ref.[1]).

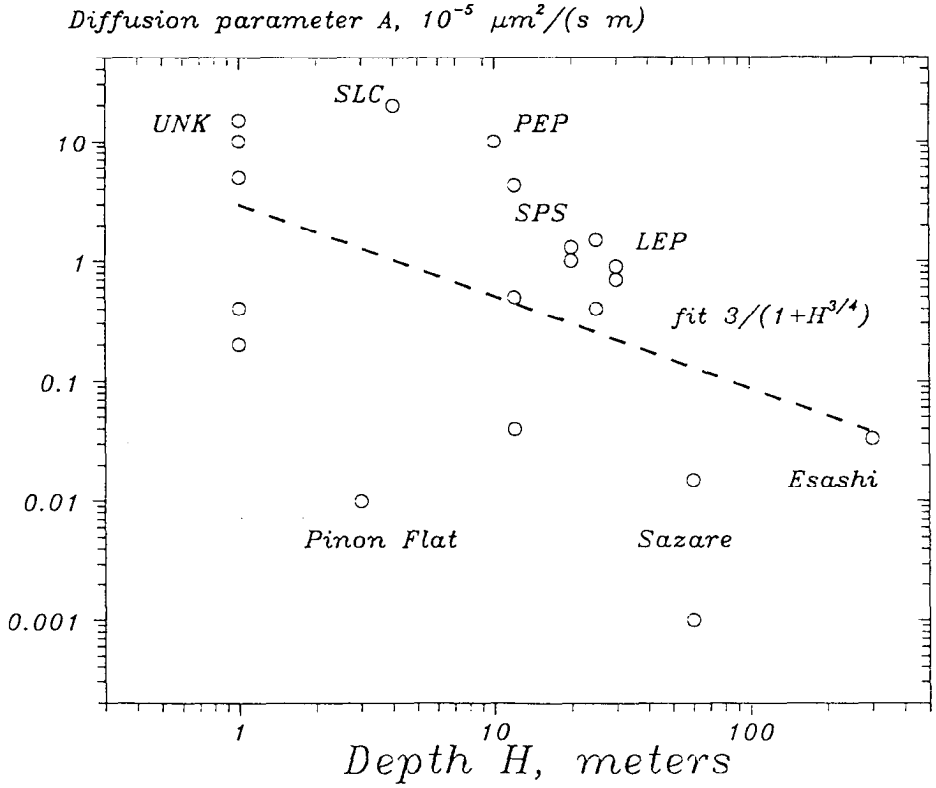

Fig.13 Diffusion parameter A vs. depth for various reported observations (see text).

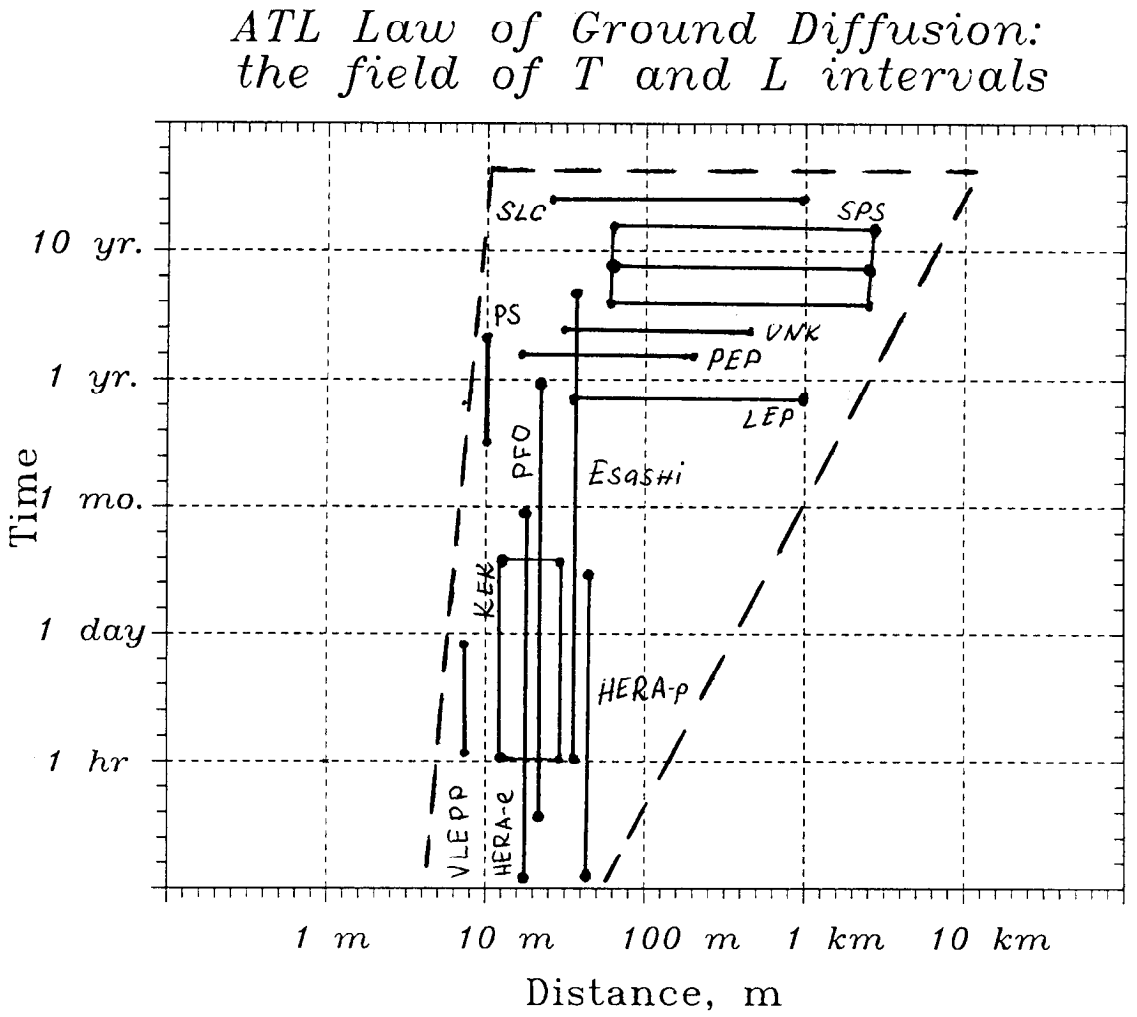

Fig.14 The intervals of T and L where the ground diffusion was experimentally detected.

Table 2: Ground diffusion observations

Site	A, $10^{-5}\ \frac{\mu m^2}{s \cdot m}$	T	L		Depth
UNK, Protvino	10	2 yr.	50–500 m	V	0 m
UNK, Protvino	10±5	1–10 hrs.	5–10 m	V, H	0 m
SLAC Linac	20±10	17 yr.	50–1000 m	V	0–5 m
SLAC PEP	10±5	20 mos.	20–200 m	V	∼10
PS pillar	0.2÷0.4	2.5 yr.	10 m	H	0 m
SPS CERN	1÷1.4	3–12 yr.	60 m – 2 km	V	∼20 m
LEP CERN	0.7÷0.9	9 mos.	40 m – 1 km	V	≥30 m
Pinon Flat	0.01	1 yr.	24 m	H	0 m
TRISTAN KEK	0.5/0.04	4 days	42.5 m/12.5 m	V	12 m
Sazare mine	0.001÷0.015	1 week	48 m	V	60 m
Esashi station	0.033±0.005	0–4 yr.	50 m	V	300 m
Orbit of TRISTAN	4.3±3	2 days	∼20 m	V	12 m
Orbit of HERA-p	1.5±1	1 s – 5 days	∼50 m	V	∼25m
Orbit of HERA-e	0.4±0.1	. s – 1 month	∼24 m	V	∼25 m

4.2 Validity Limits of the ATL Law

The question of the limits of applicability of the *ATL* law is still open. Fig.14 presents spatial and temporal intervals where the diffusion was observed. Without any doubt, typical L and T intervals at accelerators are within these limits - and the orbit drifts at HERA and TRISTAN have proved that. Nevertheless, obviously, the law should not work at small time intervals T for rather large separation length L due to independence of movements of the points, but only further investigations of slow drifts will allow us to clear the issue.

Concluding of this, section, I would like to mention that at the present time there are some evidences of the diffusion at much larger T - L intervals. For example, on the base of 50 years observation (1930-1980) at 12 points of Japan coast [23], there was found in [24] that besides daily and seasonal variations, the sea level (or, Japanese islands elevation) demonstrates some long-term “random walk” behaviour. Figs.15 a) b) show half-century sea level records measured at two Japan ports distanced by L =800 km.

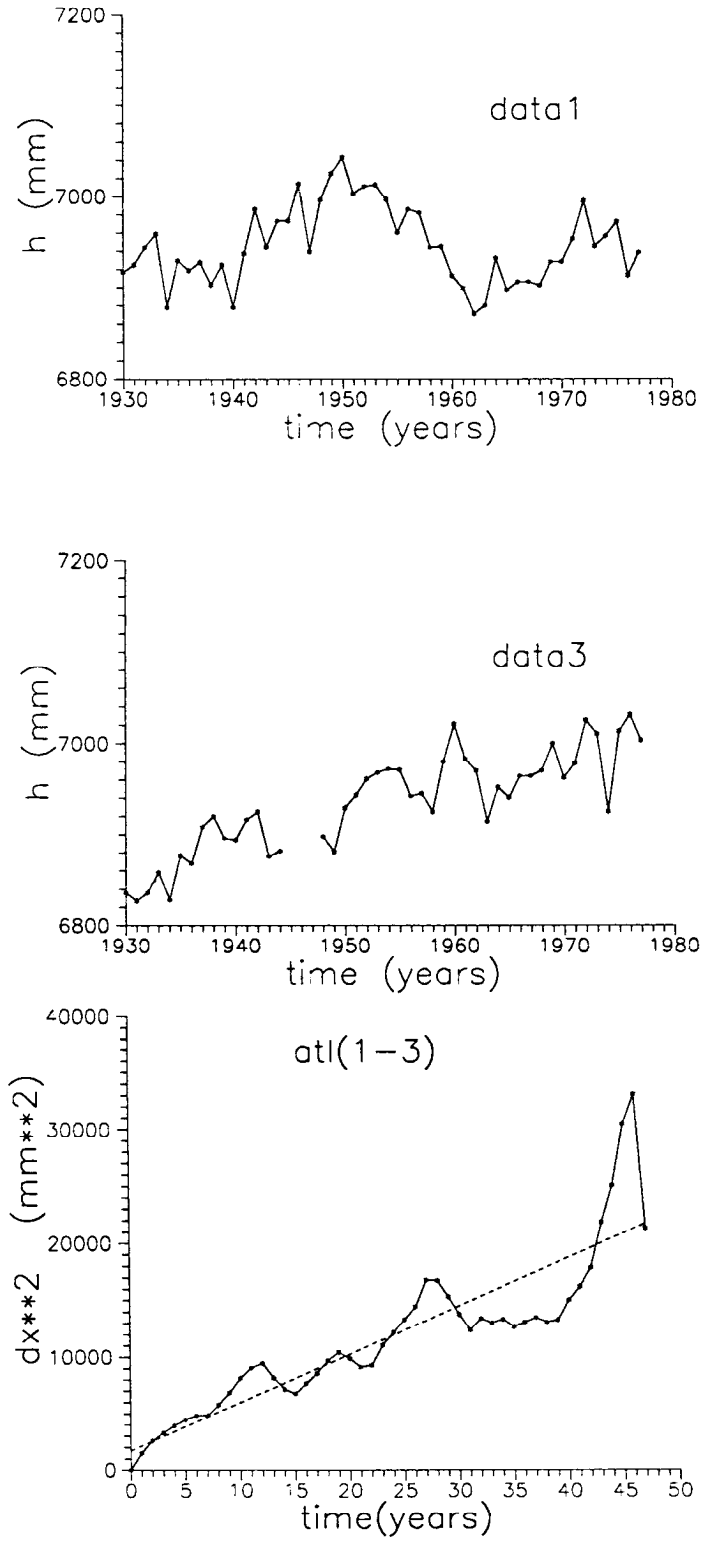

Fig. 15 Mean annual sea levels at two points of Japan coast (upper and middle plots). Lower plot shows variance of relative displacements vs. time interval T (from Ref.[24]).

Their coordinates are 32.26 N - 131.40 E and 35.09 N - 139.37 E. Calculated variance of their relative displacement versus time - see Fig.15 c) [24] - is fitted by the dashed line which corresponds to $A = 1.9 \cdot 10^{-5} \mu m^2/(s \cdot m)$. The mean diffusive coefficient for all 12 ports data was found to be $A_{Japan} = 3.5 \cdot 10^{-5} \mu m^2/(s \cdot m)$, although the L-dependence was not proved appropriately due to lack of statistics.

Another interesting result deals with power spectral density of the Earth topography (bathymetry) - see Fig.16 from [25].

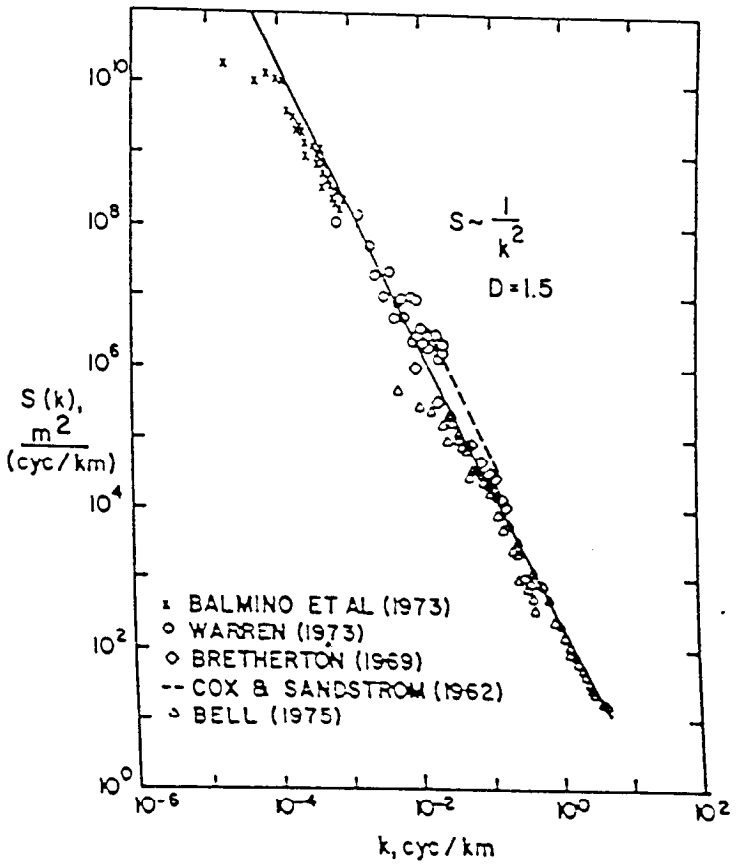

Fig.16 PSD of the earth's topography as a function of wave number. Solid line is for $1/k^2$ scaling (taken from Ref. [25]).

The compilated spectra can be approximated by $S(k) \sim [10 \div 300\ \mathrm{m}^2 \cdot km]/k^2$ where k is the wave number in [cycles/km] - in an agreement with the *ATL* prediction (3). If one assumes the coefficient A in Eq.(3) to be of the order of $10^{-4} \mu m^2/(s \cdot m)$, then the

Table 3: RMS displacement vs. time at the SSC

T	1 min	1 h	1 day	1 month	1 Yr	10 yr
$\sqrt{\langle \Delta x^2 \rangle}$	23 μm	177 μm	0.86 mm	4.7 mm	17 mm	5.2 cm
$\sqrt{\langle \delta x^2 \rangle}$	0.74 μm	5.7 μm	28 μm	0.15 mm	0.54 mm	1.7 mm

characteristic times for the Earth landscape can be estimated as $1.5 \div 50$ million years that looks reasonable.[2]

4.3 Impact of the Diffusion on Future Accelerators

In Ref.[15] some estimations were made for the longest ever started Superconducting Super Collider (USA). Using Eq.(l) with $A = 10^{-4} \mu m^2/(s \cdot m)$, we had computed the displacement of the closed orbit at the SSC. The following SSC parameters were used: β = 100 m, $\mu = \pi/4, \beta_F$ = 305 m, β_D = 54 m, C = 87120 m, F_0 = 64 m, l = 90 m, v = 122.265. The rms displacement of the closed orbit $\sqrt{\langle \Delta x^2 \rangle}$ is presented in Table 3 for different time intervals T, along with the rms value of the relative displacement of two neighboring quadrupoles $\sqrt{\langle \delta x^2 \rangle} = \sqrt{ATl}$.

Comparison of these results with the ability of the SSC correctors to displace the orbit in the ring had shown that after a period of time of l-2 years one may expect that in several $FODO$ cells the maximum correction strength will not suffice to compensate "locally" the accumulated misalignment. There was emphasized in [15] that "local" correction of the beam orbit does not return it to the original position, but instead makes it pass through the current centers of (displaced) quadrupoles. An attempt to keep the initial orbit in its original form would result in its shift relative to the center of the vacuum pipe and a substantial decrease of the dynamic aperture after only 4 months of operation.

The ATL allows to make some estimations for presently developing projects. Let us take, for example, 27-km long Large Hadron Collider (LHC) which is now under con-

[2] At the other extreme, there is a well known phenomenon of a diffusion of molecules on a crystal surfaces that leads to mean squared creeping magnitude dX growing with time T as:

$$< dX^2 >= 2DT. \qquad (17)$$

If one tries to apply the ATL law (1) for estimation of the surface diffusion coefficient $D = AL/2$, then for $L \approx$ 100 Angstrom it gives $D \approx 0.5 \cdot 10^{-4} A^2/s$ [26]. Experimental observations of Sb dimers diffusion on the (011) Si crystal surface [27] made with use of scanning tunnel microscopy has resulted in $D = 10^{-4 \pm 1}$ A^2/s at a room temperature - wonderful coincidence, although, it may have no relation to the ground diffusion.

Table 4: RMS orbit drifts vs. time at the LHC

	beam size	1 min	1 hour	1 day	1 week	1 month	1 year
rms COD	~200 μm	8 μm	60 μm	300 μm	800 μm	1.7 mm	5.7 mm

Table 5: Emittance dilution time at Linear Colliders

	CLIC	VLEPP	JLC	NLC	SBLC	TESLA
Quad. misalignment, σ_{1-to-1}	0.5 μm	0.2 μm	5 μm	4 μm	20 μm	50 μm
Quad. spacing L_Q	$\sim$ 5 m	$\sim$ 5 m	$\sim$ 10 m	$\sim$ 20 m	$\sim$ 20 m	$\sim$ 30 m
$T_d = \frac{\sigma^2_{1-to-1}}{A \cdot L_Q}$, $A = 10^{-5}\ \frac{\mu m^2}{s \cdot m}$	$\sim$ 1.5 hr.	$\sim$ 20 min	$\sim$ 3 day	$\sim$ 1 day	$\sim$ 3 weeks	$\sim$ 3 mos.

struction at CERN. Table 4 presents estimations of rms COD in the LHC in accordance with Eq.(8). The value of $A = 10^{-5}\mu m^2/(s \cdot m)$ - that we found from the LEP and SPS alignment data - was used for the estimations with time periods of 1 min, 1 hour, 1 day, 1 week, 1 month and 1 year.

Orbit drift values are compared with the beam size in arcs. The some mm COD in the LHC during 1 year should be seriously perceived as possible machine performance degradation factor.

In a high energy linear accelerators, the principal factors of luminosity reduction are beam-beam separation at the IP and emittance dilution. Beam-beam separation is an issue only if it varies from pulse to pulse (i.e. within some (dozen) milliseconds), otherwise feedback system can be used to achieve full beam's overlapping at collision.

Direct application of the *ATL* law at time intervals of about 1 s gives an estimate of the rms beam-beam displacement of the order of 10 nm (we used Eq. (9) with beta function at the IP $\beta^* \simeq$ 1 mm, number of betatron oscillations in a linac $\nu \sim 100$, and $A = 10^{-5}\mu m^2/(s \cdot m)$). This separation is comparable with the vertical beam size at the IP for all LC projects, nevertheless, we should emphasize that the diffusive model is

not quite applicable for pulse-to-pulse jitter calculations because it overestimates ground motion amplitudes at frequencies above 1 hz (see discussion on validity of the model and Fig.11).

Typically, at proposed Linear Colliders, the IP feedback can effectively keep the separation within limits at frequencies less than some (dozen) Hz, and therefore, can eliminate the effect.

Bare tolerances on quadrupole misalignments for present LC projects were calculated in Ref.[28] assuming 25% emittance dilution and simple local *"1-to-1"* correction. These values are presented in the first row of Table 5. At the same Table we also show the expected time interval after which one will need to perform linac realignment. This time was estimated as $T_d = \frac{\sigma_1^2}{A \cdot L_Q}$ where L_Q denotes approximate mean spacing between quadrupoles (the spacing can vary along the linac).

One can see from the Table 5, that in all designs the alignment tolerances are extremely tight. The expected time between realignment looks as severe requirement for the CLIC and VLEPP projects, while estimates for the JLC and NLC are somewhat relaxed. For the SBLC and, especially, for the TESLA design these requirements are quite ease and within limits of presently available technology.

Acknowledgments

I am sincere thankful to Boris Baklakov, Aandrey Sery, Vasily Parkhomchuk, Pave1 Lebedev, Valery Lebedev, Alexander Sleptsov, Sergey Savin, Gennady Stupakov, Joe Weaver, Joerg Rossbach, and Cristoph Montag for collaboration in the field of theory and experiments concerning ground motion impact on accelerators which resulted in numerous publications reviewed here.

I acknowledge many years of cooperation with Shigeru Takeda, Jean-Pierre Quesnel, Reinhard Brinkmann, and Noboru Yamomoto. They supplied me with various data which also were discussed in this article.

The pursue on the ATL law diffusion was triggered by Vasily Parkhomchuk of Novosibirsk INP and for me it has been a pleasure to work with and learn from him.

I am indebted to Susan Wipf for reading the manuscript and numerous corrections.

References

[1] B.A. Baklakov, P.K. Lebedev, V.V. Parkhomchuk, A.A. Sery, A.I. Sleptsov, V.D. Shiltsev, "Investigation of Correlation and Power Characteristics of Earth Surface Motion in the UNK Complex Region", Preprint INP 91-15, Novosibirsk (1991); see the same authors in *Proc. of 1991 IEEE Particle Accel. Conf.,* San-Francisco (1991).

[2] B.A. Baklakov, P.K. Lebedev, V.V. Parkhomchuk, A.A. Sery, A.I. Sleptsov, V.D. Shiltsev, "Study of Seismic Vibrations for the VLEPP Linear Collider", *Tech. Phys., v.38,* p.894 (1993), *(Zh. Tech. Fiz., v.63,* No.10, p.122 (1993).

[3] V. Parkhomchuk and V. Shiltsev, “Fractal Model of Ground”, Preprint INP 92-31, Novosibirsk (1992, in Russian), and *Proc. of Int. Workshop on Linear Colliders*, Garmish-Partenkirchen, Germany (1992).

[4] G.E. Fischer, “Ground Motion and Its Effects in Accelerator Design”, SLAC-PUB-3392 Rev. (1985) and AIP Conference Series No. 153, *Summer School on High Energy Particle Accelerators*, Batavia (1984).

[5] S. Takeda, H. Nakanishi, K. Kudo and A. Akiyama, “Vertical Displacement of the Base in TRISTAN”, *Proc. of HEACC’1992*, p.406, Hamburg (1992).

[6] V. Jouravlev, A. Sery, A. Sleptsov, W. Coosemans, G. Ramseier and I. Wilson, “Investigation of Power and Spatial Correlation Characteristics of Seismic Vibrations in the CERN LEP Tunnel for Linear Collider Studies”, CERN-SL/93-53 and CLIC-Note-217 (1993).

[7] V.D. Shiltsev, “Ground Motion Measurements at the SSC”, *Accelerator Physics at the Superconducting Super Collider*, AIP Conference Proceedings 326, pp.560-589 (1995).

[8] S. Takeda, K. Kudo, Y. Funahashi, A. Akiyama, and Y. Kanazawa, “Slow Ground Motion and Alignment System”, *Proc. of EPAC’94*, p. 2564, London (1994), and KEK Preprint 94-48 (1994).

[9] V. Shiltsev, B. Baklakov, P. Lebedev, C. Montag, and J. Rossbach, “Measurements of Ground Vibrations and Orbit Motion at HERA”, DESY-HERA-95-06 (1995), see also the same authors in *Proc. of 1995 IEEE Part. Accel. Conf.*, Dallas (1995).

[10] S. Takeda, A. Akiyama, K. Kudo, H. Nakanishi, and N. Yamomoto, “Slow Drifts and Frequency Spectra on Ground Motion”, KEK Preprint 93-61, and *Proc. of III Intern. Workshop on Accelerator Alignment*, Annecy, France (1993).

[11] F. Wyatt, “Displacement of Surface Monuments: Horizontal Motion”, *Journ,. of Geophys. Research*, vol. 87, No. B2, pp.979-989 (1982).

[12] V. Shiltsev, R. Stiening, “SPS Data on Tunnel Displacements and the ATL Law”, SSCL-Preprint-505 (1993).

[13] A. Sery, 0. Napoly, “Influence of Ground Motion on the Time Evolution of Beams in Linear Colliders”, DAPNIA/CEA 95-04, Saclay, and DESY Print, TESLA 95-19 (1995).

[14] J.Rossbach, “Closed-Orbit Distortions of Periodic FODO Lattices Due to Plane Ground Waves”, *Particle Accelerators*, vol.23, p.121 (1988).

[15] V. Parkhomchuk, V. Shiltsev and G. Stupakov, “Slow Ground Motion and Operation of Large Colliders”, *Particle Accelerators*, vol. 46, No. 4, pp.241-258 (1994), and SSCL-Preprint-470 (1993).

[16] National Astronomical Observatory Mizusawa, “Continuous Observation of Crustal Movements at the Esashi Earth Tides Station”, in *Report of The Coordinating Committee for Earthquake Prediction,* vol. 53, p.187, edited by Geographical Survey Institute, Ministry of Construction, Japan (1995).

[17] M. Haubin, M. Mayoud, J.-P. Quesnel, A. Verdier, “Realignment of LEP in 1993-1994”) CERN SL/94-44, and *Proc. of EPAC’94,* p. 2555 (1994);
data files are provided by J.-P. Quesnel.

[18] R. Brinkmann and J. Rossbach, “Observation of Closed Orbit Drift at HERA Covering 8 Decades of Frequency”, *Nucl. Instr. and Methods,* vol. A350 (1994), No. l-2, p.8 and DESY-HERA 94-04 (1994).

[19] J. Gervaise and E.J.N. Wilson, “High Precision Geodesy Applied to CERN Accelerators”, *1987 CERN Accelerator School: Applied Geodesy for Particle Accelerators,* CERN 87-01, p.128 (1987).

[20] V. Shiltsev, “Diffusive Ground Motion at CERN and Overview of the ATL Law Experiments”, *Proc. 1995 Int. Workshop on Linear Colliders,* KEK, April 1995 (to appear).

[21] H. Koiso, S. Kamada and N. Yamamoto, “Observation of Changes of the COD in TRISTAN Main Ring”, *Particle Accelerators,* v.27, p.71 (1990).

[22] G.E.Fischer, in *Summary and Presentation of the Workshop on Vibrational Control and Dynamic Alignment Issues at the SSC,* ed., H.J.Weaver, SSC Laboratory Special Report SSCL-SR-1185 (1992).

[23] “Monthly and Annual Mean Heights of Sea Level”, Vol.3 Japan, “Permanent Service for Mean Sea Level”, Institute of Oceanographic Sciences, Bidston Observatory, Birlenbent, Merseyside L43 7RA, UK (1978).

[24] S. Savin, “Check of the ATL Law in the Sea Level Observations”, Diploma Thesis, Novosibirsk University, Novosibirsk (1995).

[25] D.L. Turcotte, “Fractals in Geology and Geophysics”, in book of C. Scholtz, B. Mandelbrot, eds., *“Fructuls in Geophysics”,* Birkhauser Verlag, Base1 (1989).

[26] V.V. Parkhomchuk and V.D. Shiltsev, “Seismics and Accelerators”, *Sibirsky Fizichesky Journal,* No.2, p.39 (1995)) Novosibirsk (in Russian).

[27] Y.W. Mo, “Direct Determination of Surface Diffusion by Displacement Distribution Measurements with Scanning Tunneling Microscopy”, *Phys. Rev. Lett.,* vol. 71, No. 18, p.2923 (1994).

[28] T.O. Raubenheimer, “The Preservation of Low Emittance Flat Beams”, *Proc. of IEEE PAC’93, Washington,* vol.1, p.11 (1993).